Wetting and drying transitions at a fluid-wall interface. Density-functional theory versus computer simulation. II

Frank van Swol
Department of Chemical Engineering, University of Illinois, Urbana, Illinois 61801

J. R. Henderson
School of Chemistry, University of Leeds, Leeds LS2 9JT, United Kingdom
(Received 27 July 1990)

This paper reports on studies of wetting phase behavior and interfacial structure of square-well fluid adsorbed at square-well walls. Choosing a particular wetting isotherm at bulk liquid-vapor coexistence, we present our final and complete comparison between molecular-dynamics (MD) simulation and weighted-density-approximation (WDA) density-functional theory. The properties of wall-liquid, wall-vapor, and liquid-vapor interfaces are measured and used to determine contact angles and to locate the positions and order of interfacial phase transitions (wetting and drying). Due to the presence of a suitable collective mode, it was possible to directly observe the collective dynamics of the fluctuation-induced first-order drying transition in MD simulation. A practical implementation of contact-angle measurement by generalized WDA density-functional theory is detailed, enabling one to input the bulk equation of state as a boundary condition. An attempt is made to gauge the generality of our results by comparison with simulation data from other systems and with alternative versions of WDA theory.

I. INTRODUCTION

In a previous paper,[1] hereinafter referred to as paper I, we reported on a comparison between molecular-dynamics (MD) simulation data[2] and weighted-density-approximation (WDA) density-functional theory,[3] for the nature of states of adsorption at a wall-liquid interface in the presence of bulk liquid-vapor coexistence. The comparison yielded good agreement for the density profile structure and interfacial free energy (or contact angle θ) whenever the wall was at least moderately wet ($\cos\theta > -0.5$). However, this agreement broke down completely in the approach to the drying transition at low values of the wall-fluid attractive well depth (ε_W). Namely, WDA theory predicted critical drying (a second-order interfacial phase transition) at much lower ε_W than the position of the apparently first-order drying transition observed with MD simulation. Since this conflict appeared to indicate the existence of interesting physics not present in the mean-field WDA theory, it was concluded that a more complete comparison of the drying transition region was called for. In particular, (i) extensive additional simulation data were needed to pin down the order of the transition and to investigate the nature of associated fluctuation events, and (ii) a careful WDA study of transitions to dry walls required a generalization of WDA theory to enable the accurate modeling of both wall-liquid and wall-vapor interfaces simultaneously (see Sec. II below). A short report of part of this additional work has recently been published,[4] focusing on observations of dramatic collective fluctuations accompanying the first-order drying transition seen in MD simulation. This present paper describes in detail the methods and results of these extended investigations.

In Sec. II below we propose a generalization of WDA density-functional theory applied to wall-fluid wetting phenomena, to enable the direct input of the desired bulk equation of state. This is followed by a discussion of some of our conclusions concerning the nature of the WDA theory, based partly on experience obtained from projects not reported on here. In Sec. III we present a large amount of new MD simulation data on a particular isotherm of square-well fluid at a square-well wall, including a more detailed pictorial description of the collective phenomena reported earlier.[4] In addition, new results from both simulation and WDA theory are used to present a complete comparison covering the entire spectrum from complete drying to complete wetting. The paper concludes with a discussion (Sec. IV) in the context of previous and current work on simple molecular models of wall-fluid wetting phenomena.

II. WDA THEORY OF WALL-FLUID INTERFACIAL PHASE TRANSITIONS

Here, we use the phrase "WDA theory" to denote a class of mean-field excess-free-energy functionals defined in terms of a separation of the bulk equation of state into a hard-sphere term (HS) and an attractive interaction term (a) and two associated coarse-grained density profiles ($\bar{\rho}_{\rm HS}, \bar{\rho}_a$):

$$F^{\rm ex}[\rho] = \int d1\, \rho(1)[\Delta\psi_{\rm HS}(\bar{\rho}_{\rm HS}(1)) + \Delta\psi_a(\bar{\rho}_a(1))] , \quad (1a)$$

$$\bar{\rho}_i(1) \equiv \int d2\, \rho(2) w_i(12, \bar{\rho}_i(1)), \quad i \in \{\rm HS, a\} \quad (1b)$$

where $\Delta\psi = \Delta\psi_{\rm HS} + \Delta\psi_a$ denotes the excess free energy per particle of a homogeneous fluid (of density ρ) and the $w_i(12,\rho)$ are density-dependent weight functions (usually

restricted to homogeneous fluid forms). More general coarse-grained density-functional theories have been proposed,[5] including a rigorous formulation for inhomogeneous one-dimensional systems,[6] but versions of the class (1) have proved to yield both practical and accurate routes to a now extensive list of inhomogeneous fluid problems. The impressive success of WDA theory applied to wall-liquid interfaces lies in the ability of the coarse-grained density profiles to smooth strong oscillatory structure present in the true profile whenever dense fluids pack up against a solid surface or a boundary wall. For systems at bulk liquid-vapor coexistence, this situation corresponds to fairly wet substrate-fluid interfaces ($\cos\theta > 0$). When applied to wall-fluid interfaces WDA theory is defined by a grand ensemble potential functional (Ω) of the form

$$\Omega = F^{\rm ex}[\bar{\rho}] + kT\int d1\,\rho(1)\{\ln[\Lambda^3\rho(1)]-1\} + \int d1\,\rho(1)[v(1)-\mu] \tag{1c}$$

where Λ denotes the translational de Broglie wavelength, (μ, T) are the bulk thermodynamic fields (chemical potential, temperature), and $v(1)$ is an external field used to define the wall-fluid interaction (hence the use of the term wall, rather than solid). Solutions of WDA theory are obtained by minimizing Ω with respect to density fluctuations, which in practice means numerically solving an integral equation for the density profile obtained from functional differentiation of Eq. (1) with respect to ρ. In earlier versions of WDA theory much effort was placed on the HS contribution to the grand potential; in particular, expressions for the hard-sphere weight function were derived by demanding that the homogeneous fluid hard-sphere direct correlation function be accurately modeled by the second functional derivative of (1a) with respect to ρ. This emphasis on the hard-core correlations was a natural consequence of the development of WDA theory to address dense fluid packing problems at confining boundaries. In contrast, the attractive fluid-fluid correlations have tended to be treated in strict mean field:

$$\Delta\psi_a(\rho) = -\tfrac{1}{2}\alpha\rho, \quad \alpha \equiv -\int d\mathbf{r}\, u_a(r)\,, \tag{2a}$$

$$\bar{\rho}_a(1) = -(1/\alpha)\int d2\,\rho(2)u_a(r_{12}) \tag{2b}$$

where $u_a(r)$ denotes the attractive part of the intermolecular pair potential [see Eq. (2) of paper I for the precise definition of $u_a(r)$]. A more accurate approach, but qualitatively similar, is to use an equation of state obtained from bulk fluid perturbation theory;[3(b)] e.g.,

$$\Delta\psi_a(\bar{\rho}_a(1)) = \tfrac{1}{2}\int d2\,\rho(2)u(r_{12})g_{\rm HS}(r_{12},\bar{\rho}_a(z_1))$$

where $u(r)$ is now the total intermolecular potential and $g_{\rm HS}$ denotes a hard-sphere radial distribution function.

For the study of wetting phenomena in the presence of bulk liquid-vapor coexistence the WDA methods described above all possess a qualitative flaw, to varying degrees of quantitative significance. Namely, the simplified choices made for the attractive interaction contribution, $\Delta\psi_a$, all impose an unwanted approximate bulk equation of state. From this it follows that one cannot enforce desired values for both the saturated liquid density (ρ_L) and vapor density (ρ_V), simultaneously. For the comparison of paper I, the WDA temperature was chosen to fix ρ_L at the value observed by simulation, but then ρ_V was significantly different from the desired simulation value which in turn affected the wall-vapor surface free energy. Clearly, to model a contact-angle measurement properly one needs to be able to obtain wall-liquid (WL) and wall-vapor (WV) surface free energies at specified values of the bulk fluid boundary conditions. In fact, when written in the condensed form of Eq. (1) it is obvious that WDA theory is precisely of this class of theory; i.e., formally, T, μ, and $\Delta\psi(\rho)$ are all boundary conditions. Accordingly, we have investigated various choices for the attractive contribution to Eq. (1), with the view of using WDA theory in conjunction with a choice of $\Delta\psi$ fitted to bulk simulation data. Ideally, one would adopt the same approach used for the hard-sphere term in the free energy; namely, fix $\Delta\psi$ and determine $\bar{\rho}$ [i.e., $w(12,\bar{\rho})$] from knowledge of the two-body direct correlation function of homogeneous fluid. However, there does not yet exist sufficient readily available data on two-body correlations in model fluids with attractive pair interactions to make such a procedure feasible in general. One exception to this is the weak-gas limit of a pair-potential fluid; i.e., using Eq. (1) to calculate

$$\frac{\delta^2 F^{\rm ex}}{\delta\rho(1)\delta\rho(2)} \underset{\rho\to 0}{\longrightarrow} -kT(e^{-u(r)/kT}-1)$$

we find, when $u(r)$ contains a hard-sphere contribution for $r < \sigma$,

$$w_a(r,\bar{\rho}_a) \underset{\rho\to 0}{\longrightarrow} \frac{H(r-\sigma)(e^{-u_a(r)/kT}-1)}{\int d\mathbf{r}\,H(r-\sigma)(e^{-u_a(r)/kT}-1)} \tag{3}$$

where H denotes the Heaviside step function; $H(x) = (0,1)$ for $(x<0, x>0)$. However, the use of (3) in WDA theory is not appropriate to systems containing inhomogeneous regions of dense fluid. In particular, this choice of $\bar{\rho}_a$ led to excessive amounts of oscillatory structure being present in wall-liquid interfaces and even led to nonphysical liquid-vapor profiles displaying spurious oscillatory structure on the liquid side of the interface. Further investigations showed that WDA theory is highly sensitive to the choice of attractive weight function. For example, when applied to a simple liquid-vapor interface, where the two coarse-grained densities must be qualitatively similar to $\rho(z)$, the choice $\bar{\rho}_a = \bar{\rho}_{\rm HS}$ led to a totally unphysical result for $\rho(z)$ in that it contained a large peak within the liquid side of the interface.[7] Thus it is essential that the details of the attractive coarse-grained density (i.e., its gradient, interfacial width, etc.) be appropriate to the correlations present in true models. The success of WDA theory based on a strict mean-field attractive contribution, (2), is therefore a reflection of the well-known empirical observation that thermodynamic properties of dense fluids are remarkably well modeled by assuming a strict mean-field character ($g=1$) for the attractive intermolecular correlations. Thus in the absence of precise knowledge concerning the true correlations it would be foolish to depart from the choice (2b) for $\bar{\rho}_a$,

outside the weak-gas limit. Given this result, the one remaining question to answer is how sensitive is WDA theory to the chosen form of $\Delta\psi_a$? Here, we were impressed by the stability of WDA theory based on (2b) to the choice of bulk equation of state. For example, provided one makes comparisons at a fixed value of the bulk liquid density ρ_L, we observed that results for wall-liquid density profiles are remarkably insensitive to the choice of $\Delta\psi_a$. Thus we conclude that no harm is done by using a bulk equation of state fitted to simulation data, at least when WDA theory is applied to the study of wall-fluid interfaces. Finally, to ensure the best possible description of dry walls, we invoked a simple switch to enable $\bar{\rho}_a$ to change over to the weak-gas result (3) in the low-density limit. Namely, we set

$$w_a(r,\rho)=f(\rho)w_a^{\mathrm{MF}}(r)+[1-f(\rho)]w_a^{\mathrm{WG}}(r) \tag{4}$$

where the superscript MF refers to choice (2b), superscript WG refers to (3), and the switching function $f(\rho)$ was taken to be $f(\rho)=\rho/(\rho+0.05)$, with ρ in hard-core units. This simple form for $f(\rho)$ was used because when combined with (4) and (1b) the resulting $\bar{\rho}_a$ is determined by a quadratic equation involving $\bar{\rho}_a^{\mathrm{MF}}$ and $\bar{\rho}_a^{\mathrm{WG}}$. Similarly, this choice of $f(\rho)$ leads to a straightforward integral equation upon functional differential of the grand potential, i.e., yields a readily implemented generalization of Eq. (5) of paper I.

Our choice of bulk equation of state was determined by the division inherent in Eq. (1) and by the need to be able to fit simulation isotherms possessing a relatively modest amount of MD data. In fact, the following method turned out to be surprisingly robust and easy to implement. We set

$$\Delta\psi(\rho)/kT=\Delta\psi_{\mathrm{HS}}(\rho)/kT+C_1\rho+C_2\rho^2+C_3\rho^3+C_4\rho^4+C_5\rho^5 \tag{5}$$

where the HS term was taken to be Carnahan and Starling's result, as in Ref. 3(a). For a specific isotherm, the coefficient C_1 was fixed by enforcing the correct second virial coefficient, which ensured that our equation of state was a good approximation along the gas phase branch ($\rho<\rho_V$). Two of the remaining four coefficients on the right side of Eq. (5) were fixed by the conditions for bulk liquid-vapor equilibrium (i.e., $p_L=p_V$, $\mu_L=\mu_V$) at the simulation values of the coexisting densities (ρ_L,ρ_V). This left just two conditions with which to fit the liquid branch of the isotherm; namely, we fitted (5) to two reasonably spaced values of $p(\rho)$ obtained from previously published simulation data on the isotherm of interest.[8] The above procedure generated a good fit to the entire gas and liquid branches and in addition produced a simple van der Waals–like loop inside the two-phase region. Note, this latter property is required in order to be able to implement a mean-field theory such as Eq. (1). A similar analysis has also been made for two isotherms of cut and shifted Lennard-Jones (LJ) fluid. In all cases, the resulting bulk equation of state was a completely successful fit to simulation data and in addition joined the gas and liquid branches together with a perfectly reasonable van der Waals loop.

Full details of the derivation of our latest version of WDA theory and the associated numerical solution procedures are essentially as given in paper I. In particular, the functional differentiation used to obtain Eq. (5) of paper I is immediately applicable to the generalized functional Eq. (1). No changes were made to the numerical solution methods; for example, see paper I for a discussion of the WDA procedure one adopts to identify the order of interfacial phase transitions and, in the case of first-order wetting transitions, to map out the metastable and unstable free energy versus order parameter loops. It is also worth drawing attention to the links with statistical mechanical sum rules. Namely, paper I highlights the fact that WDA theory is a faithful implementation of the compressibility route to the statistical mechanics of inhomogeneous fluids, apart from the exception of a few pathological choices of weight function. This is important because the compressibility route focuses attention on the key "thermodynamic" fields relevant to interfacial physics; i.e., μ and the set of parameters defining the external field v. Isothermal derivatives of the grand potential with respect to these fields generate valuable sum rules for free-energy derivatives and interfacial compressibilities.[2] In addition, paper I shows explicitly that WDA theory satisfies hydrostatic equilibrium; as it must do since the compressibility route can be used to derive the virial route to statistical mechanics, via potential distribution theory.[9] Thus, in the presence of strong external fields, such as are used in the study of wall-fluid interfaces, WDA solutions are tightly constrained by statistical mechanics to yield physically relevant interfacial structure. We have made extensive use of this statistical mechanics both to test the numerical stability of our WDA methods (as described in paper I) and to provide a framework for direct comparison with MD simulation data (Sec. III).

To conclude this section, let us attempt to summarize what we have learned about the nature of WDA theories of contact-angle measurement, both from this current study and from projects concerning LJ fluids at LJ walls.[10] The picture that has emerged is that WDA theory is essentially determined by the boundary conditions; i.e., $v(z)$ and ρ_L and/or ρ_V. For example, the generalized theory described above gave little change to the results presented in paper I for the properties of wall-liquid interfaces,[11] because ρ_L was the same in both studies. Invariably, comparison with MD simulation shows that WDA theory is an accurate route to the structure and free energy of wall-fluid interfaces, provided large-scale collective fluctuation events have not intervened to alter the qualitative nature of the interface observed in simulation. The final component needed to generate a contact angle is the liquid-vapor (LV) interfacial tension (γ_{LV}):

$$\gamma_{LV}\cos\theta=(\Omega_{WV}^{(s)}-\Omega_{WL}^{(s)})/A \tag{6}$$

where $\Omega^{(s)}$ denotes a surface-excess grand potential defined by a Gibbs dividing surface of area A. Here, the significance of boundary conditions to WDA theory is

particularly striking. Namely, all WDA theories applied to liquid-vapor interfaces with the same boundary values ρ_L and ρ_V will essentially yield the same result for γ_{LV}. One consequence of this fact is that when using WDA theory in conjunction with a bulk equation of state fitted to real data (i.e., simulation) the results for γ_{LV} will be markedly higher than found in pure mean-field WDA theory at the same temperature (at least beyond the triple point region) because realistic equations of state possess much flatter liquid-vapor coexistence curves in the T-ρ plane. That is, the critical exponent β is about 0.32 rather than the mean-field value of $\frac{1}{2}$ and this widening of the coexistence region persists almost all the way to the triple point. The interfacial thickness is also directly related to WDA values of γ_{LV}; the steeper the interfacial gradient the higher the liquid-vapor surface tension. Our experience has therefore forced us to conclude that there is little justification in the appealing picture that a WDA liquid-vapor profile is just an MD simulation profile without capillary-wave fluctuations;[4] instead, one finds that depending on the choice of bulk equation of state (i.e., on the value of $\rho_L - \rho_V$) WDA theory predicts liquid-vapor surface tensions (with corresponding interfacial thicknesses) that are sometimes smaller (larger) and sometimes larger (smaller) than observed in MD simulation. The overall conclusion is that for a specific wetting isotherm generalized WDA theory can generally be relied on to give an accurate account of *WL* and *WV* properties but that this need not be accompanied by a good description of the associated *LV* interface.

III. SQUARE-WELL FLUID AT A SQUARE-WELL WALL

A. Drying transition revisited

When the generalized WDA theory described above was applied to the square-well wetting isotherm at $kT=\varepsilon$ (ε the fluid-fluid attractive well depth), we observed essentially the same comparison with MD data as reported in paper I. In particular, the improvement achieved in the description of WDA theory *WV* interfaces did not alter the striking disagreement over the position and apparent order of the drying transition. Accordingly, we decided next to carry out an extensive MD simulation study of the drying transition region to see if we could understand the origin of this disagreement. Altogether, in this region alone we collected simulation averages totaling 28.7 ns of real time measured in argon units.[12] Here, we adopted identical simulation procedures to those described in Ref. 2 and reviewed in paper I, to collect density profiles [$\rho(z)$] and pressure tensor component profiles [$p_N(z), p_T(z)$]; in planar geometry the transverse component of a pressure tensor [$p_T(z)$] provides a direct route to free-energy density [see Eq. (8) below]. Very briefly, the simulations were carried out at fixed $T=\varepsilon/k$ and fixed $N=512$, using systems half filled with liquid and half filled with vapor. To study drying we took an external field $v(z)$ consisting of a square-well wall (of depth ε_W and range $\sigma/2$) on the left side of the system and a hard wall boundary at the far side. These walls each had an area of $48.6038\sigma^2$ and were separated by 32.1σ of fluid.

Our account of the drying transition observed with MD simulation has been published in letter form,[4] and it is not our intention to repeat these observations here; rather, we wish to take this opportunity to present a more pictorial discussion of data briefly described in Ref. 4. Two key sets of results were presented in Ref. 4: (i) simulation data on a metastable partially dry branch that subsequently collapsed to complete drying and (ii) observations of dramatic collective fluctuations preceding and initiating the drying transition. Figure 1 below shows the wall-liquid density profiles belonging to the stable and metastable states whose histories and adsorptions are listed in Table I of Ref. 4. These five states are clustered around the drying transition which lies within the range $0.925 \le \varepsilon_W/kT \le 0.95$. Here, the lower limit is set by the highest value of ε_W at which we observed a collapse to complete drying while the upper limit is a guess based on indications that the $\varepsilon_W=0.925$ system lies very close to the transition point [see below and see also the analysis based on Eq. (7) shown in Fig. 4 below]. Of the five partially dry systems shown in Fig. 1, two subsequently underwent transitions to completely dry states (the bottom profile in Fig. 1) but only after long periods of metastable behavior interspersed with transient large-scale fluctuations in adsorption (an example is shown in Ref. 4); other systems not appearing in Fig. 1 underwent transitions at much earlier stages in their simulation.[4] When these histories are taken into account the metastability so clearly illustrated in Fig. 1 is conclusive evidence for the first-order nature of the drying transition seen in our simulation systems. A complementary view of this conclusion may be based on a statistical-mechanical sum rule for the slope of the wall-liquid surface-excess grand potential ($\Omega_{WL}^{(s)}$), which is particularly clear cut in our square-well

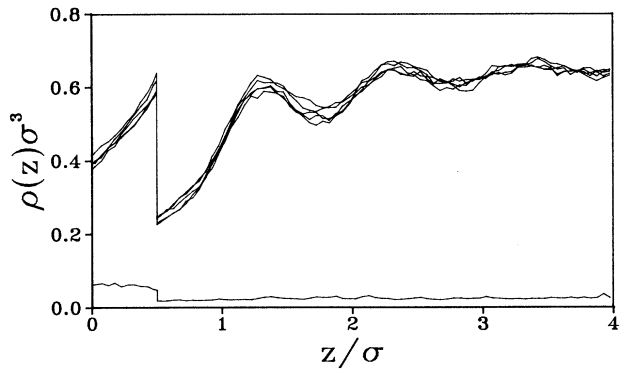

FIG. 1. Wall-liquid density profiles at bulk liquid-vapor coexistence for square-well fluid at a square-well wall, in the vicinity of the drying transition belonging to the isotherm $kT=\varepsilon$. The five partially dry profiles came from 1.2 ns averages within metastable and stable periods of systems at $\varepsilon_W/kT=0.875$, 0.925, 0.95, 0.95, and 0.97, respectively (see Table I of Ref. 4). The two systems at lowest ε_W subsequently underwent transitions to completely dry states; the bottom profile shown above.

model:[2]

$$\frac{\partial \Omega_{WL}^{(s)}/A}{\partial \varepsilon_W} = -\int_0^{\sigma/2} dz\, \rho_{WL}(z) \tag{7}$$

where $\sigma/2$ is the chosen range of our attractive square-well external field (of depth ε_W). That is, the contrast between the values of the right side of Eq. (7) corresponding to the stable and metastable profiles of Fig. 1 with that belonging to a completely dry wall (the bottom curve of Fig. 1) is a direct signature of the first-order nature of the transition; namely, it implies a discontinuous derivative of the free energy with respect to the relevant thermodynamic field.[13] In contrast, WDA theory yields a continuous spectrum of density profiles as ε_W is lowered towards the drying transition, as appropriate to a second-order transition (so-called critical drying).

The simulation system at $\varepsilon_W/kT=0.925$, hereinafter referred to as the $\varepsilon_W/kT=0.925$ system, was studied for an especially lengthy period; 48×10^6 particle collisions or 14.8 ns of argon time. This arose because, unlike with three previous collapses observed at lower values of ε_W, the $\varepsilon_W/kT=0.925$ system initially yielded transitions to dry walls which subsequently jumped back to the metastable branch. A description of the lengthy history of this system is as follows: (1) beginning from a starting configuration generated at $\varepsilon_W/kT=0.95$, the $\varepsilon_W/kT=0.925$ system was first equilibrated for a period of 0.92 ns; (2) there then followed a lengthy display of metastable behavior lasting for 3.4 ns, occasionally interrupted by fluctuations leading to the transient creation of an adsorbed layer of gas of up to 1.5σ in thickness (such fluctuations occurred on a time scale of around 0.2 ns); (3) the $\varepsilon_W/kT=0.925$ system was then observed to collapse to a dry state in which the liquid film was separated from the left-hand wall by 5.5σ of vapor; however, around 0.5 ns later, fluctuations in the center of mass of the 16σ long liquid film had returned the system to a state of relatively high adsorption (the metastable branch); (4) there then followed a second lengthy period of metastable behavior, this time lasting for 3.7 ns; (6) at this point the $\varepsilon_W/kT=0.925$ system underwent a spectacular dynamic event, illustrated in Fig. 3 below, in which during a large 1.2 ns subaverage it spent about 0.5 ns in a relatively wet state and a similar amount of time in a state with 6σ of vapor adsorbed at the wall, interspersed by two large collective leaps of the liquid film; (7) further runs continued totaling an additional metastable period of 5.5 ns, until finally an unequivocal transition to a completely dry state suddenly occurred (see Fig. 2 below).

For a more detailed picture of the nature of the large-scale collective motions associated with the first-order MD drying transition, let us focus on aspects (6) and (7) of the history of the $\varepsilon_W/kT=0.925$ system. Figure 2 displays the very last 0.92 ns of the simulation life of this system, ending with the final and complete transition to a dry *WL* interface. Two aspects of the drying transition are immediately apparent from Fig. 2; namely, the suddenness of the onset of the transition and the dramatic speed of the subsequent motion of the liquid film. The same behavior was seen in other systems whose wall-

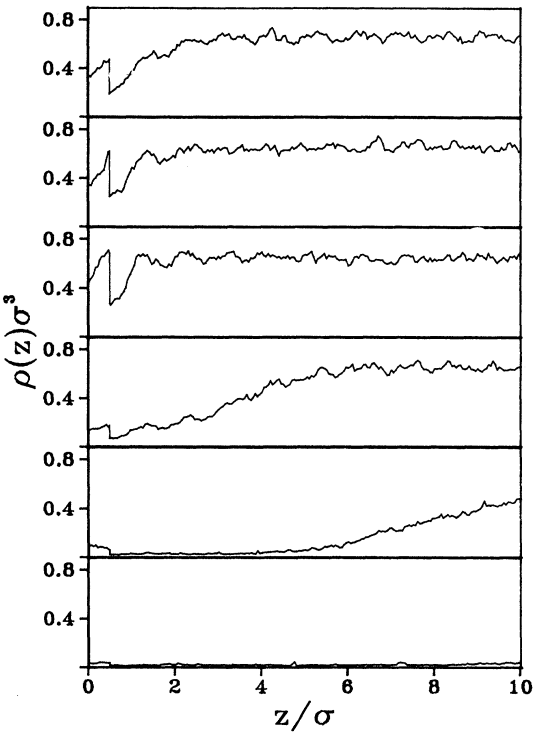

FIG. 2. The final 0.29 ns of the simulation life of the $\varepsilon_W/kT=0.925$ system. The profiles show six subaverages of equal length ordered sequentially from top to bottom.

liquid profiles collapsed to dry walls and by being careful to maintain identical double precision simulation procedures (for example, identical lookup tables) it was possible to repeat these transition events to collect profiles over much shorter subaverages. From Fig. 2 and other examples we observe a typical peak collective velocity of about 0.032σ ps^{-1}, which corresponds to the center of mass of the liquid film moving 1σ during the time its constituent particles have each undergone about 400 collisions. Put another way, under these special circumstances each liquid atom is traveling on average 7% faster in the direction away from the left-hand wall than in other directions. Presumably, this collective velocity is representative of the temperature, the number of particles, and the dimensions of our simulation systems. The dramatic events captured in Fig. 3 highlight the apparently chaotic nature of these large-scale collective motions; i.e., the strong bimodal character of the pressure profile is the result of two sudden jumps of the entire liquid film. The first of these leaps created an adsorbed layer of vapor 6σ in thickness, which lasted for about 0.5 ns before the system jumped back again to a relatively wet state. This ability to move back and forth across the free-energy barrier is suggestive of a weak first-order phase transition and is probably also indicative of the presence of finite-size dynamics. In fact, from the work of Binder and others,[14] given an interfacial area of the size used in our study one would expect a non-self-averaging diffusive $k=0$ mode to dominate the collective motion of the liquid film whenever the adsorbed layer of

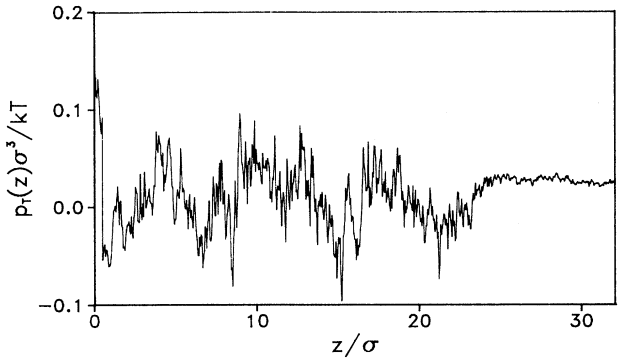

FIG. 3. The transverse component of the pressure tensor during a 1.2 ns subaverage of the $\varepsilon_W/kT=0.925$ system. The strong bimodal character of the pressure profile, note the presence of three liquid-vapor interfaces, captures the essence of two dramatic collective events (see text).

gas is beyond about 5σ thick. As well as the case shown in Fig. 3, a $k=0$ mode was occasionally observed subsequent to an unequivocal transition to a completely dry state; in particular, one liquid film did a little dance in the center of the system whereby it suddenly reversed its direction of motion and traveled 1.5σ back towards the attractive wall, before reversing its direction again one last time to carry on and eventually collide with the far boundary wall. It remains an open question as to how great a role (if any) this $k=0$ diffusive mode plays in initiating the first-order drying transition observed in our MD simulations.

Additional details of possible significance concerning the collective dynamics of our systems include the following: (i) we commonly noted that just prior to a collapse the adsorption climbed briefly to a relatively high peak, suggesting that the transition is actually initiated by a fluctuation in the opposite direction which quickly falls back to such an extent that the system cannot maintain its metastable partially dry state; (ii) the interfacial area is only just large enough to support observable capillary-wave modes, but interestingly an analysis[8] of the *WL* interface of the $\varepsilon_W/kT=0.925$ system just prior to its collapse (the third profile in Fig. 2) showed evidence of a $[\cos(2\pi x/L)+\cos(2\pi y/L)]$ capillary-wave-like distortion that was not present under normal circumstances; (iii) alteration in round-off errors to the double precision arithmetic destroyed the repeatability of any specific collective drying transition event; i.e., these instabilities are not stable to numerical round-off error.[15]

To sum up the above discussion, let us repeat our conclusion reported in Ref. 4 that the contrast between the dynamical events observed in MD simulation and the smooth second-order behavior seen in WDA theory suggests that in our MD systems the transition to complete drying is an example of a fluctuation-induced first-order phase transition, possibly influenced by finite-size dynamics.

B. Simulation data and comparison with WDA theory

Table I lists some of the most significant wall-liquid interfacial data collected from our new simulation studies

TABLE I. MD simulation data for wall-liquid interfaces along the isotherm $kT=\varepsilon$. System denotes a particular MD simulation run or series of subaverages (see text). ε_W is the wall-fluid attractive well depth. Γ_{WL} denotes adsorption at a wall-liquid interface (Ref. 2); a representative error is ±0.05. $\Omega^{(s)}$ denotes surface-excess grand potential, directly measured from pressure tensor profiles; a representative error is ±0.06. The final column gives data for the right-side of sum rule (7); average error is ±0.015. DT denotes data associated with the drying transition point, obtained by combining results from five systems clustered around $\varepsilon_W/kT=0.93$; here, the surface grand potential value is that defined by complete drying together with the *WV* and *LV* interfacial free energies (see text). DGp and WGp distinguish the drying-group and wetting-group systems at $\varepsilon_W/kT=1.5$; see text.

System ε_W/kT	$\Gamma_{WL}\sigma^2$	$\Omega^{(s)}_{WL}\sigma^2/kTA$	$(\partial\Omega^{(s)}_{WL}/\partial\varepsilon_W)\sigma^2/A$
DT, 0.93	−0.38	0.22	−0.24
1.0	−0.32	0.19	−0.27
1.125	−0.17	0.13	−0.34
1.25	−0.09	0.03	−0.38
1.375	−0.10	0.09	−0.39
DGp, 1.5	−0.07	−0.03	−0.44
WGp, 1.5,	−0.03	0.03	−0.45
1.75	0.02	−0.01	−0.51
1.875	0.01	−0.10	−0.51
2.0	0.06	−0.30	−0.54
2.25	0.13	−0.33	−0.58
2.5	0.16	−0.44	−0.60

of square-well fluid adsorbed at square-well walls. The systems belong to two distinct groups; namely, a drying group (DGp) and a wetting group (WGp). At low values of ε_W, up to and including the DGp $\varepsilon_W/kT=1.5$ system, the simulation procedures were identical to those of our previous studies.[1,2] Here, we were able to avoid the necessity to simulate attractive wall-vapor interfaces (little useful data could be collected here anyway due to the small number of particles on the vapor side of a system) because of the availability of a more accurate theoretical route. However, this method rules out direct study of a wetting transition at the *WV* interface. Accordingly, to investigate the wetting side of the interfacial isotherm, we modified our simulation procedures as follows: (i) the external field was symmetrized so that both the right-hand and left-hand walls were now square-well potentials; then by using identical well depths and maintaining the asymmetric *WL-LV-WV* nature of the profiles (as used in the DGp simulations) we could simultaneously collect data on all three interfaces;[16] (ii) the length of the simulation box was extended from 32.1σ to 48σ, which would be essential if a wetting transition was to occur on the right-hand wall since then the system would need to be able to accommodate two strongly structured *WL* interfaces together with two relatively high-temperature *LV* interfaces; to maintain appropriate amounts of bulk fluid, N was increased from 512 to 990 particles.

Table II lists data belonging to wall-vapor interfaces. Here, direct data are restricted to the wetting group of simulations. The comparison between the weak-gas (WG) theoretical limit[17] and WDA theory results for the

TABLE II. Properties of wall-vapor interfaces along the isotherm $kT=\varepsilon$. See caption to Table I. The column headed MD shows direct simulation data, WG is the weak-gas limiting result (Ref. 17), and WDA denotes the density-functional theory of Sec. II.

System ε_W/kT	$\Omega^{(s)}_{WV}\sigma^2/kTA$ MD	WG	WDA
DT, 0.93		−0.025	−0.020
1.0		−0.028	−0.023
1.125		−0.034	−0.029
1.25		−0.041	−0.036
1.375		−0.049	−0.044
DGp, 1.5		−0.057	−0.053
DWGp, 1.5	−0.06	−0.057	−0.053
1.75	−0.01	−0.079	−0.078
1.875	−0.09	−0.091	−0.095
2.0	−0.14	−0.105	−0.115
2.25	−0.12	−0.140	−0.175
2.5	−0.11	−0.185	−0.265

same isotherm shows that the contribution to WV properties arising from many-body correlations may be ignored on the drying side of a wetting isotherm (i.e., for $\cos\theta<0$). The wetting transition seen in WDA theory is first order with a surface free-energy barrier of $0.023kT/\sigma^2$, although accompanied by a large increase in the WV adsorption just prior to the transition. Our conclusion from a fairly extensive search by simulation is that it is unlikely that one could ever directly observe a first-order wetting transition with our MD simulation methods. That is, none of our systems showed any significant tendency to increase the WV adsorption beyond the WG profile, even when the value of ε_W belonging to the right-hand wall was increased to a ludicrous value. Here, the problem was not so much a lack of transport through the gas phase but rather the single-particle nature of this transport; i.e., the contrast between the drying and wetting behavior observed in MD simulation is presumably due to the absence of an appropriate collective mode in our wetting systems. At the first-order drying transition we clearly observed large-scale collective fluctuations in the WL adsorption capable of carrying the system over the weak first-order barrier to complete drying. However, with our choice of simulation geometry the only route to complete wetting of a WV interface is accretion of particles from the bulk liquid via single-particle transport through the vapor phase, which gave every indication of being a totally inadequate mechanism when confronted with a first-order barrier.[18] Although we were not able to study the dynamics of wetting, this failure itself strongly indicates that the transition is first order.

All of the simulation data presented here are new results. In fact, three partial wetting systems presented in Ref. 2 and paper I were repeated, to ensure consistency throughout the isotherm and to increase the level of statistical accuracy. In Tables I and II, the drying group results were obtained from averages over 4×10^6 collisions (1.2 ns in argon units), apart from those labeled DT, for drying transition, which combine all the stable and metastable systems whose density profiles appear in Fig. 1. For the wetting group we used runs of 6×10^6 collisions (0.9 ns) except for the $\varepsilon_W/kT=2.25$ and 2.5 systems which were averaged for twice this period. Further simulations at much higher values of ε_W, searching for but failing to observe a dynamical wetting transition, are not shown. Also absent from these tables are data from the extensive series of simulations searching for drying transitions beyond the metastable states of DT. The new data are everywhere consistent with our previously published results,[2] for both interfacial properties and bulk fluid properties. With regard to the latter: (i) The bulk LV coexistence pressure belonging to the isotherm was measured as $p\sigma^3/kT=0.0258\pm0.0006$ from 22 ns of drying group and drying transition simulations, and $p\sigma^3/kT=0.026\pm0.002$ from 7.2 ns of wetting group simulations; in addition, we always collected the full profile of the normal component of the pressure tensor $[p_N(z)]$ to check for hydrostatic equilibrium within wall-fluid interfaces and across the coexisting regions of bulk liquid and vapor. (ii) Simulation values for the saturated liquid density were $\rho_L\sigma^3=0.6495\pm0.0012$ from 17.3 ns of drying group and drying transition simulations, and $\rho_L\sigma^3=0.647\pm0.004$ from 7.2 ns of wetting group simulations. (iii) The wetting group yielded a direct MD mea-

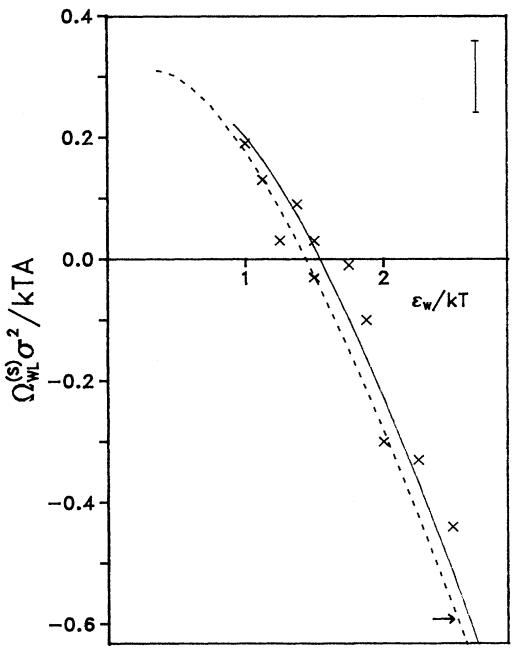

FIG. 4. Surface-excess grand potential per unit area of wall-liquid interface of square-well fluid at a square-well wall, along the isotherm $kT=\varepsilon$ at bulk liquid-vapor coexistence. The crosses show raw simulation data obtained from pressure tensor component profiles (third column of Table I); a representative error bar is given at top right corner. The solid curve follows from a fit to the simulation data for sum rule (7); the final column in Table I; combined with the observed position of the drying transition and the measured liquid-vapor surface tension (see text). The dashed curve is the prediction of WDA theory, beginning top left at the position of the second-order WDA drying transition; a horizontal arrow marks the first-order wetting transition seen at the WDA wall-vapor interface.

sure of the vapor density; $\rho_V\sigma^3=0.034\pm0.003$, which is in good agreement with known virial coefficients and the bulk pressure measured throughout our systems.[8]

Figure 4 summarizes the latest results for the surface-excess grand potential of *WL* interfaces along our wetting isotherm, spanning all states from complete drying to complete wetting. The large statistical error present in the raw MD data is representative of direct measurements of free energy by simulation. Our experience arising from the large amount of simulations carried out in this and related projects indicates that the ubiquitous nature of this statistical error arises from characteristic fluctuations of the partition function of the entire system. The time scale involved here is large; in particular, it is unrealistic to expect to be able to simulate for long enough periods to significantly reduce this error in systems of our size. There is significantly less statistical error present in the derivative of a free-energy with respect to a thermodynamic field; thus the most accurate route to $\Omega_{WL}^{(s)}$ should be via sum rule (7). An obvious way to implement this latter approach is to use the results for the right side of Eq. (7) in conjunction with the measured value of the liquid-vapor surface tension and the observed position of the drying transition; i.e., $\Omega_{WL}^{(s)}$ is a continuous function of ε_W and at complete drying $\Omega_{WL}^{(s)}/A=\Omega_{WV}^{(s)}/A+\gamma_{LV}$. This route, using the final column of Table I fitted to a quadratic in ε_W, is shown as the solid curve in Fig. 4. Clearly, the comparison with WDA theory is remarkably good as far as the slope of the free-energy isotherm is concerned. From sum rule (7) we see that this arises because the *WL* density profile structure is well characterized by WDA theory; explicit results are given in Fig. 5. For completeness, we show in Fig. 6 MD simulation profiles of the transverse component of the pressure tensor $[p_T(z)]$, corresponding to the *WL* profiles of Fig. 5(b); note, the negative of $p_T(z)$ (in our case, as defined by Irving and Kirkwood[19]) is also a grand canonical potential density:

$$\Omega/A=-\int_{-\infty}^{\infty}dz\,p_T(z)\ . \tag{8}$$

Before leaving the results of Fig. 4 it should be noted that we did not find the approach based on Eq. (7) to be straightforward in practice, due to some ambiguity in the measured value of γ_{LV}. In particular, values of γ_{LV} measured outside the drying transition region appeared to be consistently higher than that corresponding to the observed position of the drying transition. Namely, (i) 22 ns of drying group and metastable drying transition data, directly measured from pressure tensor profile differences, gave $\gamma_{LV}\sigma^2/kT=0.27\pm0.01$; (ii) 7.2 ns of wetting group pressure tensor data gave $\gamma_{LV}\sigma^2/kT=0.27\pm0.04$; while (iii) 18.5 ns of drying transition data for the right side of (8) implied, equating this with the grand potential of a completely dry system, $\gamma_{LV}\sigma^2/kT=0.22\pm0.03$. The solid curve shown in Fig. 4 uses the average of these two results; clearly, the highest value is the least compatible within apparent statistical error with the direct MD data, given the position of the drying transition obtained from the behavior of the order parameter (i.e., the value of ε_W where $\Omega_{WL}^{(s)}/A=\Omega_{WV}^{(s)}/A+\gamma_{LV}$). Analogous behavior has also been seen in Lennard-Jones systems belonging to a similar isotherm, but not at temperatures much closer to the triple point.[10(b)] It is conceivable that this discrepancy might be due purely to statistical error not sampled correctly even by the long simulation runs employed in this project. Alternatively, one might be tempted to invoke an influence arising from finite-size collective dynamics; namely, is it possible that additional diffusive motions of the finite-size liquid film, that must surely contribute to the complete drying states of our sys-

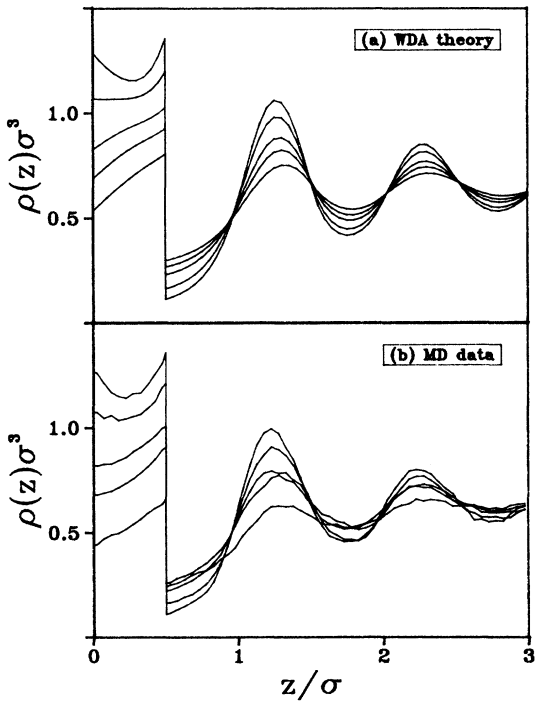

FIG. 5. Wall-liquid density profiles at bulk liquid-vapor coexistence for square-well fluid at a square-well wall, at selected points along the isotherm $kT=\varepsilon$. From highest to lowest oscillatory amplitude, the profiles belong to systems at $\varepsilon_W/kT=2.5$, 2.0, 1.5, 1.25, and 1.0, respectively. (a) WDA theory results. (b) MD simulation data.

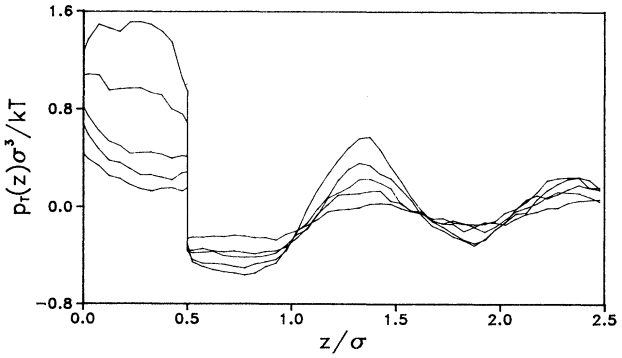

FIG. 6. MD simulation data for wall-liquid profiles of the transverse component of Irving and Kirkwood's pressure tensor, obtained from the same systems appearing in Fig. 5(b). Note the significance of Eq. (8) to these profiles.

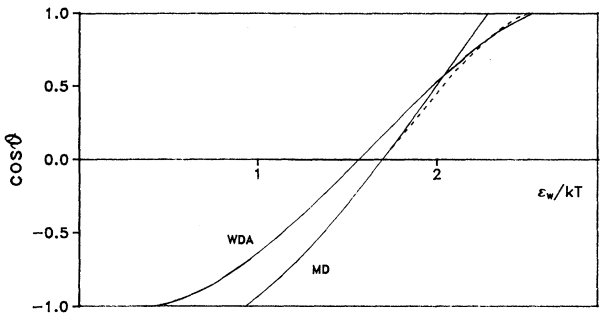

FIG. 7. Cosine of the contact angle as a function of the attractive strength of wall-fluid potential, along the wetting isotherm $kT=\varepsilon$ at bulk liquid-vapor coexistence. The solid curve labeled WDA shows the prediction of density-functional theory; beginning with zero slope at a second-order drying transition ($\cos\theta=-1$) and ending with finite slope at a first-order wetting transition ($\cos\theta=1$). MD denotes simulation results (see text); in our simulation systems both interfacial phase transitions show first-order behavior. The dashed curve uses WDA theory to estimate the probable outcome given unattainably long simulation runs (see text).

tems, are sufficient to reduce $\gamma_{LV}\sigma^2/kT$ from 0.27 to 0.22? If this latter mechanism were present then the solid curve of Fig. 4 would need to be shifted down to lie very close to the WDA prediction and the observed position of our drying transition would lie at a higher value of ε_W than appropriate to systems with macroscopic interfacial area.

In Fig. 7 we show final results for the contact angle of square-well fluid at a square-well wall, along the isotherm $kT=\varepsilon$. In plotting our MD simulation curve we have assumed the compromise value of γ_{LV} referred to above; i.e., $\gamma_{LV}\sigma^2/kT=0.245$. The solid curve labeled MD follows from our *WL* free-energy results (the solid curve in Fig. 4) in conjunction with WG theory for $\Omega^{(s)}_{WV}$ (given in Table II). The latter choice is representative of the raw simulation data on *WV* interfaces because of the single-particle nature of the transport of material across the vapor region of our systems; i.e., the majority of our *WV* interfaces never showed much progression beyond the WG limit. The dashed curve in Fig. 7 indicates the effect of replacing $\Omega^{(s)}_{WV}$ with WDA data, which is likely to yield better estimates close to complete wetting than our simulation procedures; in particular, the dashed curve ends at a first-order wetting transition fixed by taking $\Omega^{(s)}_{WV}$ to be the value belonging to WDA theory's first-order wetting transition.

IV. DISCUSSION

The above results and those of paper I, Ref. 4, and Ref. 2 present a consistent picture of the nature of wall-fluid wetting phenomena and the comparison between MD simulation and WDA theory. But, how general are these conclusions likely to be?

A positive answer to this question is provided by a recent study of cut and shifted LJ fluid adsorbed at a cut and shifted 9-3 wall,[10(b)] applying the same analysis pioneered in square-well systems. In particular, Ref. 10(b) uses MD simulation to map out five wetting isotherms spanning low temperatures relatively close to the triple point up to an isotherm slightly closer to the bulk critical point than the single temperature employed in our square-well studies. In addition, a direct comparison with WDA theory of LJ systems was made for both the highest and the lowest wetting isotherms. Qualitative differences between the observations of Ref. 10(b) and those of our square-well studies would have to reflect a sensitivity to the details of the shape of short-range wall-fluid and fluid-fluid interactions, because the simulation geometry and the WDA methods of the square-well project were deliberately matched in the LJ project. However, the results obtained from LJ systems showed a remarkable similarity with those of our square-well study; i.e., no qualitative difference was observed with any MD simulation data or WDA theory prediction. In particular, (i) both sets of simulations possessed analogous dynamical events accompanying the first-order drying transition, (ii) wetting transitions behaved similarly in both classes of systems, and (iii) WDA theory always predicted critical drying at a lower value of ε_W than the position of the first-order drying transition observed in simulation.

Perhaps the most interesting single result reported here and in Ref. 10(b) concerns the dynamical nature of the drying transition seen in MD simulation. Namely, the conclusion reported in Ref. 4 that we have directly observed a fluctuation-induced first-order phase transition. This class of weak first-order phase transition is characterized, at least in renormalization-group (RG) studies, by second-order mean-field behavior that changes order when one includes the effect of a large-scale collective mode that is missing or mistreated in mean-field theory. Such transitions are regularly discovered in complex systems and in interfacial physics,[20] and may provide a unifying link between rigorous theories of phase transitions of different order.[21] The precise nature of the collective mode observed in our simulations remains somewhat of an open question; in particular, it is unclear how significant a role the interesting phenomena of $k=0$ finite-size dynamics might be playing in our dry systems. The conclusion here is that it would be valuable to pursue these dynamical events via some nonlinear RG theory of drying transitions at a wall-fluid interface, assuming that the Landau limit agrees with our WDA theory prediction of critical mean-field behavior.

If the only recent work involving simulation studies or WDA theories of wetting phenomena at wall-fluid interfaces was restricted to those projects discussed above and in Ref. 10 (i.e., concerning work by the present authors) then we could end here by concluding that we now possess a consistent and robust understanding of wetting and drying in wall-fluid systems with short-range interactions. Unfortunately, this is not the case and we are forced instead of conclude with the following cautionary tale, that in particular concerns the drying transition region.

Firstly, the reader's attention should be drawn to a series of projects studying wetting phenomena of LJ fluid at LJ walls; hereinafter referred to as the Sikkenk *et al.*

simulations,[16] or the Nijmeijer *et al.* simulations.[22] The earlier work[16] has largely been withdrawn,[22] at least as far as the drying transition is concerned, due mainly to shortcuts used in attempts to get around problems arising from hardware restrictions inherent in the use of a special purpose LJ computer. Thus let us confine our present comments to the latest conclusions of Nijmeijer *et al.*, as found in particular in Ref. 22(b). Overall, there is close similarity between the wetting isotherms reported by us [including Ref. 10(b)] and the results of Ref. 22. However, a clear qualitative difference arises in the nature of the drying transition and associated fluctuation phenomena. In particular, the latest conclusion of Nijmeijer *et al.* concerning the drying transition is that they have all along been observing a second-order transition (critical drying). There is therefore a significant difference in the fluctuation phenomena observed by us and by Nijmeijer *et al.*; i.e., the latter do not report the existence of a metastable partially dry branch as found here and in Ref. 10(b) and thus sum rule (7) no longer implies first-order drying. However, throughout their studies Sikkenk *et al.* and Nijmeijer *et al.* have observed $k=0$ motion of the liquid film that has often been suggestive of first-order metastability, although apparently not of sufficient dominance to force the authors into recognizing the existence of a metastable branch. There are four differences between the two classes of simulation that may be responsible for the above discrepancy. (1) Differences between the wall-fluid interactions; the latest work of Nijmeijer *et al.* uses a lattice based external field representing the outer three layers of a rigid LJ solid. (2) Finite-size rounding; hardware restrictions led Sikkenk *et al.* and Nijmeijer *et al.* to use a simulation box with too small a distance between the substrate walls than is appropriate to the relatively high temperature of their wetting isotherm. In fact, the results of a separate study of LV interfaces, using the special purpose computer, clearly show that their simulation box cannot accommodate two full liquid-vapor interfaces for temperatures at and above $kT=0.9\varepsilon$[10(b),23] This raises the question of whether the failure of Ref. 22(b) to observe a clear first-order drying transition could be due to finite-size rounding of the transition, particularly as one might imagine that too small a box length would dissuade the system from generating two incomplete bulk regions of vapor and thus suppress collapses of the type shown in Fig. 2 above. (3) Finite-size dynamics; Sikkenk *et al.* and Nijmeijer *et al.* use an interfacial area approximately 16 times that involved in our work and that of Ref. 10(b), and the greater the mass of the liquid film the less significant the $k=0$ mode will be. Thus perhaps our drying transition fluctuations are induced by finite-size dynamics that is suppressed in Ref. 22. (4) Incorrect dynamical procedures; when reporting observations of critical drying Nijmeijer *et al.* emphasize that their MD procedures include a regular zeroing of the center of mass momentum of the fluid film (every 5200 time steps). This is clearly a dubious procedure to adopt in the possible presence of a fluctuation-induced first-order phase transition.

Our experience with square-well systems and LJ systems both from simulation studies and WDA theories does not support the notion that the drying transition is sensitive to details of short-range wall-fluid interactions. With regard to the remaining three possible explanations, we note that (3) is more controversial than (2) because it would amount to finite-size sharpening of a phase transition. Accordingly, we would suggest either (2) or (4) as the most likely of the above four possibilities.

Let us now turn to the predictions of WDA theory; in particular, we could not ignore a recent WDA study[24] set up to compare directly with the simulations of Sikkenk *et al.*[16] Reference 24 reported first-order behavior at the WDA drying transition. The situation was even more ironic because the WDA theory used by us has an ancestry that began as an early WDA program written by Tarazona (one of the authors of Ref. 24) for the specific study of Yukawa fluid at an exponential wall (acknowledged in paper I). In a first attempt to understand this disagreement we applied our most recent WDA program to the case of cut and shifted LJ fluid at three layers of cut and shifted 10-4 solid averaged over the interfacial plane, which is the closest one can get with a planar external field to modeling the simulation systems of Sikkenk *et al.* In complete analogy with all of our previous WDA studies we found no evidence of first-order drying, to at least two orders of magnitude smaller than the free-energy barrier reported in Ref. 24. Elsewhere along the wetting isotherm we found similar behavior to that reported in Ref. 24, although in our version the first-order WDA wetting transition has a significantly smaller free-energy barrier. However, this has been cleared up following recent correspondence between the present authors and those of Ref. 24. Velasco and Tarazona report (unpublished results) that a detailed study of the drying transitions discussed in Ref. 24 shows that they are second-order transitions; i.e., there is no evidence for first-order drying at the level of accuracy available to WDA theory. The free-energy barrier reported in Ref. 24 is actually an upper bound obtained in the absence of any minimization; at the time the authors were only interested in showing that the WDA drying transition could not be as strong as suggested by the original simulations of Sikkenk *et al.*

ACKNOWLEDGMENTS

This work was supported by a NATO Collaborative Research Grant and by a SERC grant of CRAY computer time at the UK Atlas Centre.

[1]F. van Swol and J. R. Henderson, Phys. Rev. A **40**, 2567 (1989).

[2]F. van Swol and J. R. Henderson, J. Chem. Soc. Faraday Trans. 2 **82**, 1685 (1986).

[3](a) P. Tarazona, Phys. Rev. A **31**, 2672 (1985); (b) W. A. Curtin and N. W. Ashcroft, Phys. Rev. Lett. **56**, 2775 (1986).

[4]J. R. Henderson and F. van Swol, J. Phys. Condens. Matter. **2**, 4537 (1990).

[5]See, e.g., the review by T. K. Vanderlick, L. E. Scriven, and H.

T. Davis, J. Chem. Phys. **90**, 2422 (1989).

[6]J. K. Percus, J. Chem. Phys. **75**, 1316 (1981).

[7]This confirms the suspicions of footnote 25 of paper I that oscillatory structure sometimes present in LV profiles obtained from WDA theory is linked to unphysical correlations; in particular, inappropriate treatment of fluid-fluid attractive interactions.

[8]J. R. Henderson and F. van Swol, Mol. Phys. **56**, 1313 (1985).

[9]J. R. Henderson, Mol. Phys. **50**, 741 (1983).

[10](a) J. R. Henderson and F. van Swol (unpublished); (b) P. Adams and J. R. Henderson (unpublished).

[11]Here, let us take this opportunity to correct a misprint appearing in the caption to Fig. 6 of paper I; namely, the highest-temperature isotherm plotted there belongs to $T/T_c=0.85$ not 0.93.

[12]I.e., $(m\sigma^2/\varepsilon)^{1/2}\equiv 2.16$ ps.

[13]In wetting phenomena at bulk liquid-vapor coexistence the surface field ε_W plays an equivalent role to the thermodynamic field T, provided the system does not approach a tricritical point separating first-order wetting transitions from critical wetting; see, e.g., the review by D. E. Sullivan and M. M. Telo da Gama, in *Fluid Interfacial Phenomena,* edited by C. A. Croxton (Wiley, New York, 1986).

[14]K. K. Mon, K. Binder, and D. P. Landau, Phys. Rev. B **35**, 3683 (1987); D. M. Kroll and G. Gompper, *ibid.* **39**, 433 (1989).

[15]Note that the discontinuous nature of our Hamiltonian implies that the long-time dynamics of our simulation systems is rigorously chaotic (i.e., unstable to arbitrarily small numerical error); see, e.g., R. H. G. Helleman, in *Fundamental Problems in Statistical Mechanics V,* edited by E. G. D. Cohen (North-Holland, Amsterdam, 1980).

[16]J. H. Sikkenk, J. O. Indekeu, J. M. J. van Leeuwen, and E. O. Vossnack, Phys. Rev. Lett. **59**, 98 (1987); J. H. Sikkenk, J. O. Indekeu, J. M. J. van Leeuwen, E. O. Vossnack, and A. F. Bakker, J. Stat. Phys. **52**, 23 (1988).

[17]WG limit:

$$\Omega^{(s)}_{WV}\sigma^2/kTA=-\tfrac{1}{2}\rho_V\sigma^3(e^{\varepsilon_W/kT}-1)\simeq -0.0165(e^{\varepsilon_W/kT}-1)\ .$$

In footnote 21 of paper I we describe a more sophisticated theory for WV interfacial properties, valid to higher-order in ρ_V. Such an approach is needed at very low ε_W, but is an unnecessary complication over the range of systems shown in Table II; in fact, the WG result is surprisingly good because of cancelling errors (see the comparison with WDA theory in Table II).

[18]One direct route to the thermodynamics of wetting transitions by simulation would be to adopt Monte Carlo procedures invoking nonphysical dynamics able to tunnel through the free-energy barrier, such as including a step that threw liquid atoms at the WV interface; cf. J. E. Finn and P. A. Monson, Phys. Rev. A **39**, 6402 (1989). Alternatively, one could alter the interfacial geometry to induce a suitable collective mode, such as might be expected to be present in systems containing LV menisci intersecting boundary walls [M. J. P. Nijmeijer, C. Bruin, A. F. Bakker, and J. M. J. van Leeuwen, Physica A **160**, 166 (1989)].

[19]J. H. Irving and J. G. Kirkwood, J. Chem. Phys. **18**, 817 (1950).

[20]See, e.g., B. Halperin, T. Lubensky, and S. Ma, Phys. Rev. Lett. **32**, 292 (1974); P. Tarazona and E. Chacon, Phys. Rev. B **39**, 7157 (1989).

[21]E. Domany, D. Mukamel, and M. E. Fisher, Phys. Rev. B **15**, 5432 (1977).

[22](a) M. J. P. Nijmeijer, C. Bruin, A. F. Bakker, and J. M. J. van Leeuwen, Physica A **160**, 166 (1989); this work is based on direct observation of the contact angles of curved menisci [as pioneered by G. Saville, J. Chem. Soc. Faraday Trans. 2 **73**, 1122 (1977)]; (b) (unpublished); two studies using methods analogous to our work.

[23]M. J. P. Nijmeijer, A. F. Bakker, C. Bruin, and J. H. Sikkenk, J. Chem. Phys. **89**, 3789 (1988). A plot of the coexisting liquid and vapor densities reported by these authors indicates that the bulk critical temperature of their symmetric systems lies well below 1.1ε instead of in the range 1.11ε–1.12ε which is the known result appropriate to cut and shifted LJ fluid; as confirmed by Ref. 10(b). In fact, Sikkenk *et al.* and Nijmeijer *et al.* do not appear to be aware of the true critical point appropriate to their cut and shifted (the latter is inherent in the simulation dynamics) LJ Hamiltonian, since they invariably quote $kT_c\simeq 1.26\varepsilon$. In contrast to the simulations of Sikkenk *et al.* and Nijmeijer *et al.* our square-well systems lie further away from the critical point and could readily accommodate symmetric dry states within the 32.1σ length of the drying group simulation box. Similarly, in Ref. 10(b) a box length of 34σ was used to observe the fluctuation-induced first-order drying transition at $kT=0.9\varepsilon$, which can accommodate significantly more vapor than the simulations of Sikkenk *et al.* and Nijmeijer *et al.*

[24]E. Velasco and P. Tarazona, J. Chem. Phys. **91**, 7916 (1989).